Investigating Electric Properties of WTe_2

Moira Miller*[1] and mentor Dr. David Cobden[2]

[1]Virginia Tech Blacksburg, VA 24061
[2]University of Washington Seattle, WA 98105

ABSTRACT

Van der Waals structures can be used to investigate electrical properties of two-dimensional materials. Materials in two dimensions can exhibit properties that are very different to their thicker forms. There is still much new physics to be investigated in 2D physics, including the potential ferroelectric properties of WTe_2. Ferroelectric materials display hysteresis polarization as a function of electric field, as a result of switching internal electrical dipoles. A previous WTe_2 device has seen switching, so we investigated a bilayer WTe_2 device and thick WTe_2 device to further understand these properties. We again observed switching in the WTe_2, which we were able to observe in the top gate graphene as well.

Keywords: Ferroelectric switching, shielding, semiconductor, WTe_2, 2D Van der Waals structures

1. Introduction

Two-dimensional van der Waals structures allow for the investigation and discovery of new physics in a wide variety of materials, including semi-metals (such as graphene), semiconductors, superconductors, and insulators (such as hexagonal boron nitride). Often materials exhibit unusual properties in monolayer and few layers, which can be very different to their behavior in three dimensions. Van der Waals structures are fabricated by stacking monolayer and few-layer materials using the weak van der Waals force [1]. This paper investigates the properties of WTe_2 in bilayer. Figure 1 is an image of the monolayer WTe_2 lattice structure. In monolayer the material is centro-symmetric and has inversion symmetry. In its trilayer form and above, WTe_2 acts like a semi-metal. This paper investigates the bilayer and thick forms of WTe_2.

Figure 1. Lattice structure of WTe_2. Blue is W (Tungsten) and orange is Te (Tellurium).

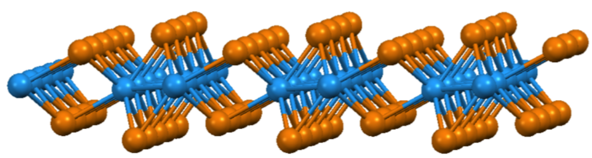

Ferroelectric materials are those with a switchable macroscopic polarization induced by a transverse electric field [2]. Ferroelectric switching is observed in a hysteresis loop in a graph of polarization versus electric field, showing the polarization tracing a different path as the electric filed changes direction. Ferroelectric properties are not expected to arise in metals, however, since free electrons are expected to screen the affect of dipole moments on the overall electrostatic forces. But our lab has observed hysteresis in a graph of conductance verses electric displacement in a previous device, as seen in Figure 2. The devices in this paper (bilayer and thick WTe_2) were investigated to further understand this phenomenon. Poles could potentially be allowed to form since WTe_2 loses its symmetry in its bilayer form.

Figure 2. Hysteresis observed in a previous WTe_2 device.

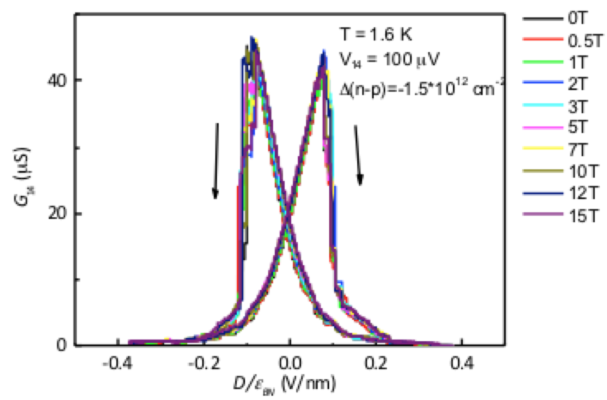

WTe_2 oxidizes in air, and so must be encapsulated to preserve its electrical properties. Figure 3 motivates encapsulation: the graph on the left is non-encapsulated trilayer WTe_2 and the right is encapsulated by hBN. The non-encapsulated material

* moira18@vt.edu

acts like an insulator, while the encapsulated WTe_2 has semi-metallic properties. Figure 4 is a diagram of the encapsulated WTe_2 and also demonstrates where the data in Figure 3 was taken.

Figure 3. Graphs of resistance versus temperature in Kelvin for trilayer WTe_2. Left is non-encapsulated; right is encapsulated by hBN.

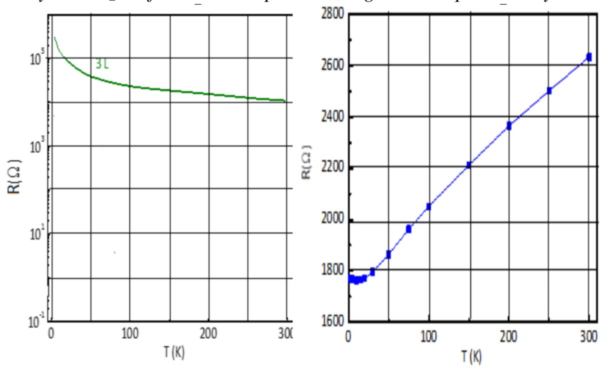

Figure 4. Diagram of WTe_2 encapsulated by hBN. Platinum contacts shown as gray squares. Current symbol demonstrates how the previous data in Figure 2 was taken.

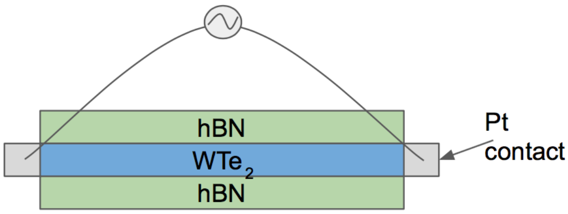

Another important feature of the van der Waals strucutres are the top and bottom gates. The gates for these devices were made from few layer graphite (FLG) bottom gates and graphene (defined to be monolayer) top gates. Having both a top and bottom gate allows for more tunability of the devices, as more parameters can be controlled. According to the following equations the electric field (or electric displacement) and carrier density may be tuned depending on the top and bottom gate voltages:

$$D \approx \frac{1}{2}(D_b + D_t) \approx \frac{1}{2}\epsilon_{BN}(\frac{V_{bg}}{d_{bg}} - \frac{V_{tg}}{d_{tg}})$$

$$\Delta(n-p) = \epsilon_{BN}(\frac{V_{bg}}{d_{bg}} + \frac{V_{tg}}{d_{tg}}).$$

By tuning both the electric field and carrier density, the van der Waals structures can study more interesting 2D physics than if there were only one variable. Figure 5 shows a van der Waals structure consisting of WTe_2 encapsulated by hBN with a graphene top gate and a FLG bottom gate.

Figure 5. The bilayer WTe_2 device. Encapsulation as seen in Figure 4, with top and bottom gates in red. Gold contacts shown on top gate.

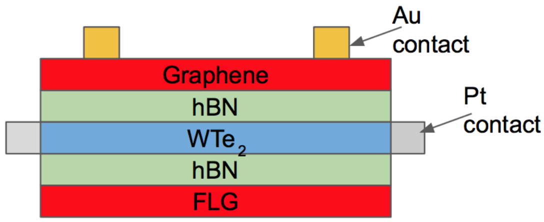

2. Materials and Methods

2.1. Exfoliation

Using the method of Scotch tape exfoliation, hBN, graphene, and graphite can be transferred onto SiO_2 chips. Figure 6 shows the Scotch tape method. First, the SiO_2 chip (top right) is cleaned. Next, tape is covered in the required crystal (top left, in this case graphene is being exfoliated), and exfoliated by opening and closing the tape to reduce the number of layers and spread out the material. Next, the tape is placed on the SiO_2 chip and smoothed to avoid bubbles (bubble visible in bottom left image). The chip and tape are heated at 100°C for 2-3 minutes. Finally, after cooling, the tape is removed and the chip is ready for searching (bottom right).

Figure 6. Clockwise from upper left: SiO_2 chip; exfoliation tape; tape pressed onto SiO_2 tape; removing the tape.

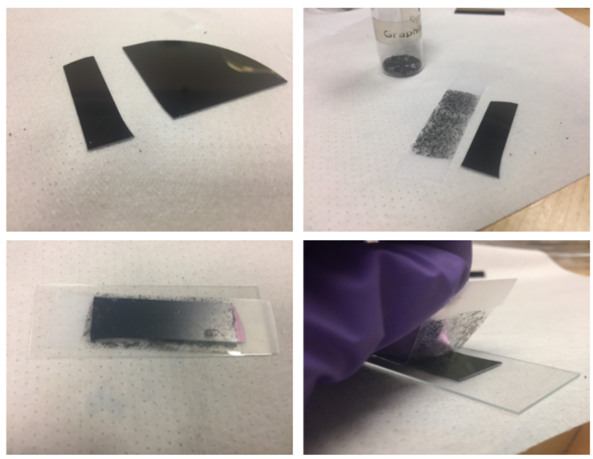

2.2. Searching

Searching is done on Olympus BX51M and Zeiss AXIO optical microscopes on the 20x magnification setting. Depending on the device being built particular shapes, sizes, and colors are preferred. Figure 7 gives an example of a graphite piece not ideal for a device, but with many features seen in these 2D layers. A monolayer graphene is visible as the pale pink triangle on the bottom, with more layers visible on the piece as well. The yellow pieces on the top right are examples of bulk graphite, which is many-layered and not used in these devices. Tape residue is marked in the bottom left of the figure.

Figure 7. Example of graphite on SiO_2. Figure demonstrates common features in searching: monolayer grahnene, multiple layers, ridges, bulk, and tape residue.

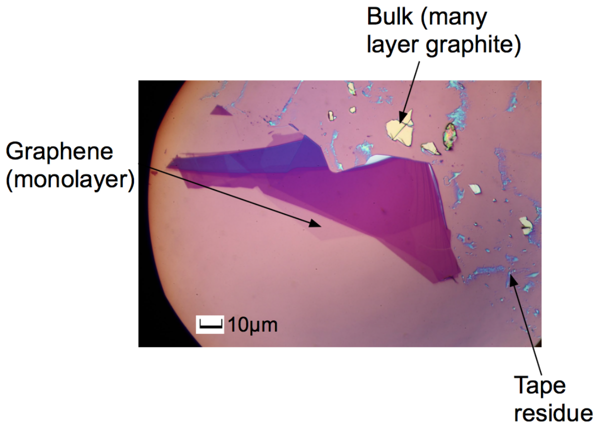

Figure 8 shows graphene (top left) and hBN (top right) pieces found in 20x magnification, and then with the magnification increased to 80x (bottom images). Once a piece is found, it is checked for obvious ridges, uneven layers, and tape residue. To better look for these features, the pieces are scanned by an Atomic Force Microscope. The cleanest pieces are chosen and arranged to have the most available space for contacts.

Figure 8. Images of searching in the optical microscope. Top two images are in 20x setting, boxes in center are area zoomed in below (80x). Bottom left is graphene piece used in thick WTe_2 device; bottom right is hBN piece used in same device. Bottom images have scale giving size of the pieces.

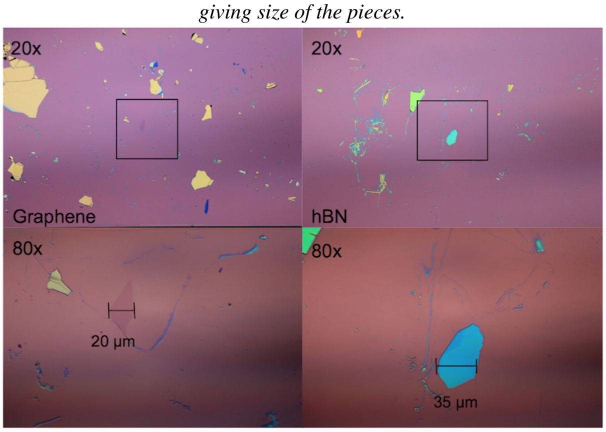

2.3. Transfers and Stamps

Once the pieces have been found and device geometry has been decided, it is time to start stacking the van der Waals structures, using the stamp transfer method. Stamps are made on glass slides using two polymers, a compressible PDMS covered with sticky PC. The right image in Figure 9 shows a zoomed-in image of the stamp. The whole stamp setup is shown in the left image. The stamp is brought down close to the piece and then the aluminum block is heated, expanding the block and bringing the stamp smoothly over the piece. After passing over the piece, the aluminum block is cooled, and the stamp retracts, picking up the piece.

Figure 9. Images of transfer setup. Left shows the optical microscope used for searching. Microscope stand has aluminum block with SiO_2 chip on top. Left side of image shows the micro-manipulator attached to the stamp. Right image zooms in on the stamp.

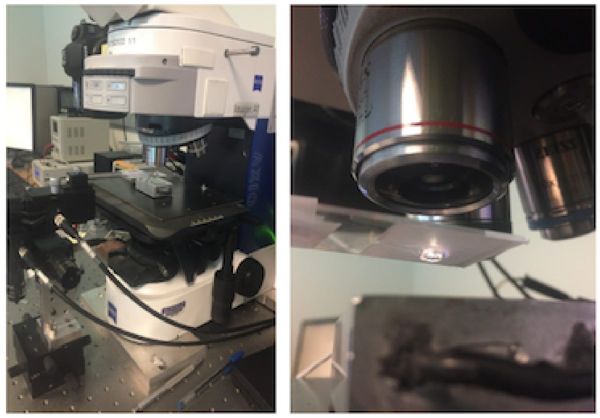

Figure 10 shows the stamps (left image) in the bottom left as it approaches a piece of few layer graphene (FLG). The hBN and graphene have already been picked up on the stamp and are visible as a white shape at the end of the FLG. The image on the right shows all three pieces on the stamp in 100x magnification. Pieces are picked up from the top down and finally melted down.

Figure 10. Left image shows the stamp (green area bottom right) as it approaches the piece of few layer graphite (purple piece in center). Picture taken in 20x. White shape by the FLG is the hBN and graphene on stamp. Right image is picture of the three pieces on the stamp in 100x. Graphene (very faint) and hBN are vertical, FLG is horizontal.

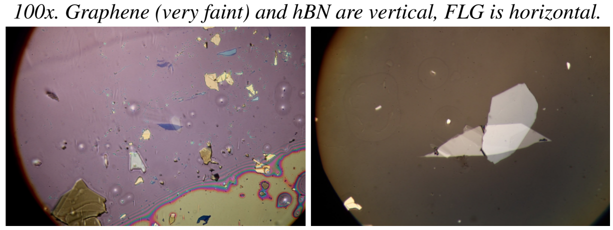

2.4. Electron Beam Lithography and Contacts

Electron Beam Lithography is used to create a pattern for the contacts on the melted-down stamp PC. The contacts will be used to probe the top gate (and, for the bilayer device, the WTe_2) as well as apply a voltage to the bottom gate. Then gold is evaporated over the device, which washes off in chloroform with the PC and remains on the contacts (see Figure 11). The square gold areas are used to connect to the wire bonds, which allow the device to be gated and probed.

Figure 11. Image of contacts on the thick device. Gold contacts come off of the top gate graphene and extend to square pads which attach to the wire bonds.

3. Results and Discussion

The devices were cooled to 4K in a cryostat, and the temperature was increases incrementally to 300K as data was being taken. Data was collected by sending a 100 mV voltage through a pair of probes and measuring the resulting current. The gate voltage was swept from -5V to 6V, creating a graph of conductance (G= I/V= 1/R) versus gate voltage.

Figure 12. Top down image of the bilayer device. The gold contacts are on the top gate graphene, and the platinum contacts are on the bilayer WTe_2.

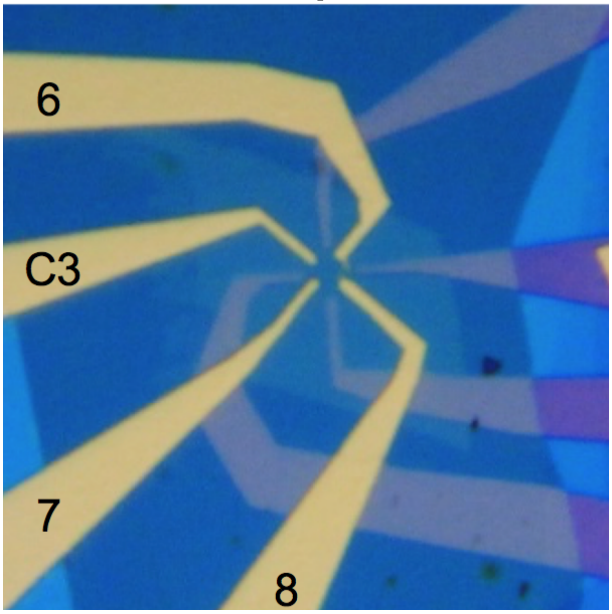

Figure 12 shows the contacts on the bilayer WTe_2 device. Figure 13 shows the graph of conductance versus gate voltage in the top gate graphene, taken by flowing a small voltage through C3 and 8, while holding 6 and 7 grounded to prevent current flowing to the contacts not being probed. In this setup V_{bg} was set to V_{WTe2}, and both were swept. The graph shows the ability of these van der Waals devices to tune the carrier density of a material, in this case the graphene. As the gate voltage changes, so does the conductance, and they are related linearly on either side of the Dirac point.

Figure 13. Conductance versus back gate voltage in top gate graphene. The V_{bg} was set to V_{WTe2}.

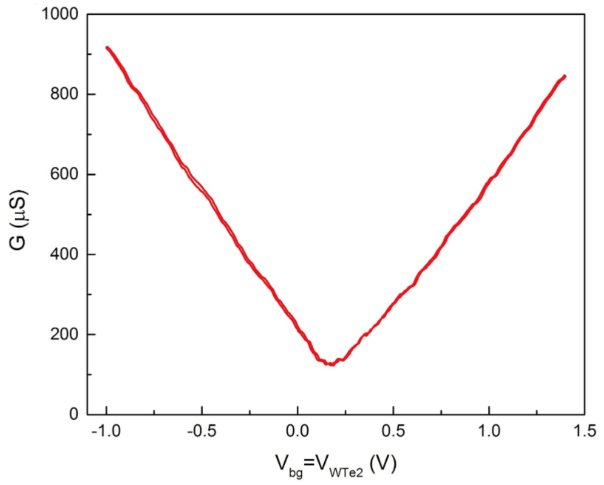

Next, the graphene was grounded, the back gate swept, and the bilayer WTe_2 was probed. Figure 14 shows the device layers and the location of probes.

Figure 14. Schematic of the bilayer device, showing voltage probe across the WTe_2 and grounded gold contacts on the graphene.

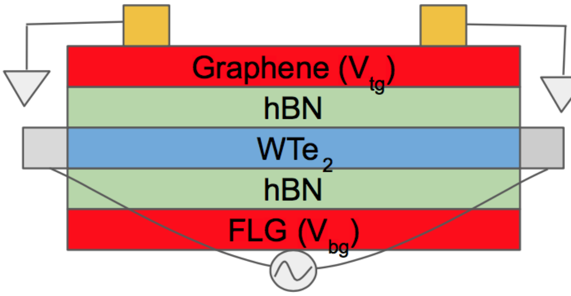

Figure 15 is a graph of conductance versus back gate for the bilayer device. Note the overall shape demonstrating similar ability to tune the number of carriers, as seen in Figure 13. There is a large hysteresis loop visible below 0V on the gate voltage, suggesting a switching of poles within the WTe_2 as a function of back gate voltage.

Figure 15. Conductance versus back gate voltage in bilayer WTe_2. The

V_{bg} was swept and the V_{tg} was grounded.

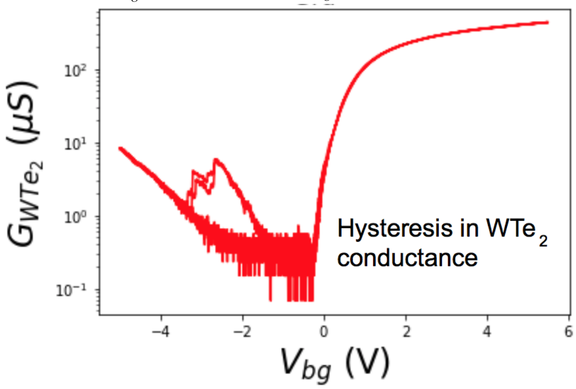

To see if a switching of poles in the WTe$_2$ affected the top gate, similar measurements were taken as above, but the WTe$_2$ was grounded, and the top gate was probed. Figure 16 shows the bilayer device with the probes and gates labeled.

Figure 16. Schematic of the bilayer device, showing voltage probe across the V_{tg} and grounded WTe$_2$.

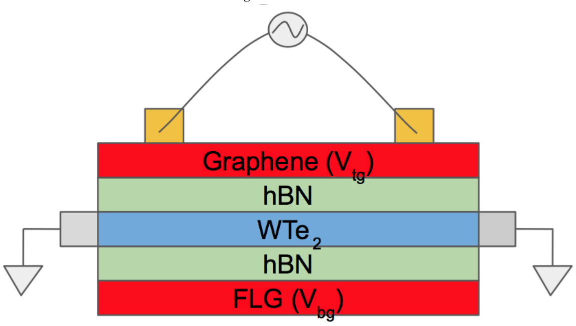

Figure 17 shows the graph of conductance in the top gate graphene versus V_{bg}. There is clearly a large hysteresis in the curve, suggesting that polar switching in the WTe$_2$ can be observed in the top gate. There is also a large lack on the overall graphene conductance versus V_{bg} shape compared to Figure 13, which also probed the graphene top gate. This suggests that the WTe$_2$ screens the top gate, and the electrical effects seen in the top gate are due to electrical properties of the WTe$_2$.

Figure 17. Conductance versus back gate voltage in bilayer top gate graphene. The V_{bg} was swept and the V_{WTe2} was grounded.

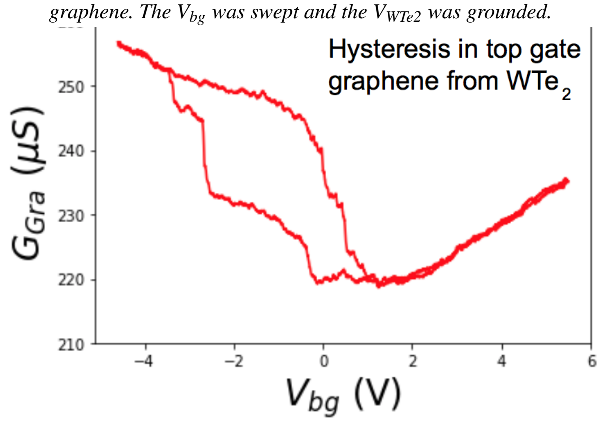

The thick WTe$_2$ did not show signs of hysteresis in the top gate in temperatures from 4K to 300K, suggesting that the top layer of WTe$_2$ does not polarize in many layer WTe$_2$.

4. Conclusions

Our results demonstrated a possible ferroelectric property of a bilayer WTe$_2$ when probed within a 2D van der Waals structure. We also demonstrated the screening affect of the bilayer WTe$_2$ on the top gate graphene. The screening was visible in thick WTe$_2$, but no ferroelectric effects were observed. Polarization of metals is counterintuitive, since the free conductance electrons screen the internal electric fields [3]. If what we are observing is indeed ferroelectric polarization and switching within the bilyaer WTe$_2$, then this phenomenon would require new theory.

5. Acknowledgments

We would like to thank Professor David Cobden for hosting me for the summer, Tauno Palomaki for his help, and the graduate students in the lab: Boris Dzyubenko, Zayao Fei, Josh Kahn, Bosong Sun, Paul Nguyen, and Wenjin Zhao.

I would like to acknowledge and thank Gray Rybka, Deep Gupta, Cheryl McDaniel, Linda Vilett, and the National Science Foundation for the opportunity to do research this summer at the University of Washington.

6. References

1. H. Liu, N. Han, J. Zhao, RSC. Adv. 5, 17572 (2015).

2. Uchino, Kenji. Ferroelectric Devices Second Edition (CRC Press, 2009).

3. Lines, M. E. and Glass, A. M. Principles and Applications of Ferroelectrics and Related Materials (Oxford Univ. Press, 2001).